EUROPEAN FUSION DEVELOPMENT AGREEMENT

EFDA–JET–CP(06)03-14

F. Ryter, Y. Camenen, J.C. DeBoo, F. Imbeaux, P. Mantica, G. Regnoli,
C. Sozzi, U. Stroth, ASDEX Upgrade, DIII-D, FTU, TCV, Tore Supra,
W7-AS Teams and JET-EFDA Contributors

Electron Transport Studies

Electron Transport Studies

F. Ryter[1], Y. Camenen[2], J.C. DeBoo[3], F. Imbeaux[4], P. Mantica[5], G. Regnoli[6], C. Sozzi[5], U. Stroth[7], ASDEX Upgrade, DIII-D, FTU, TCV, Tore Supra, W7-AS Teams and JET-EFDA Contributors*

[1]Max-Planck-Institut für Plasmaphysik, EURATOM Association, D-85748 Garching, Germany
[2]Centre de Recherches en Physiques des Plasmas, Ecole Polytechnique Fédérale de Lausanne, Association EURATOM-Confédération Suisse, CH-1015 Lausanne, Switzerland
[3]General Atomics, PO Box 85608, San Diego, California 92186-5608, USA
[4]Association Euratom - CEA, CEA/DSM/DRFC, CEA Cadarache, 13108 Saint Paul lez Durance Cedex, France
[5]Istituto di Fisica del Plasma, Associazione EURATOM-ENEA-CNR, 20133 Milano, Italy
[6]Associazione Euratom-ENEA sulla fusione, Via E. Fermi 44, 00045, Frascati, Italy
[7]Institut für Plasmaforschung, Universität Stuttgart, Pfa enwaldring 31, 70569 Stuttgart, Germany

**Fusion Energy 2000 (Proc. 18th Int. Conf. Sorrento, 2000), IAEA, Vienna (2001).*

Preprint of Paper to be submitted for publication in Proceedings of the
33rd EPS Conference,
(Rome, Italy 19-23 June 2006)

“This document is intended for publication in the open literature. It is made available on the understanding that it may not be further circulated and extracts or references may not be published prior to publication of the original when applicable, or without the consent of the Publications Officer, EFDA, Culham Science Centre, Abingdon, Oxon, OX14 3DB, UK.”

“Enquiries about Copyright and reproduction should be addressed to the Publications Officer, EFDA, Culham Science Centre, Abingdon, Oxon, OX14 3DB, UK.”

ABSTRACT

Electron transport in fusion plasmas is intensively studied. Great progress in physics understanding has been achieved during the last years and the main recent results are reviewed here. In particular, it appears that a threshold in normalised gradient explains most of the observations, both in steady-state and transient conditions. Comparisons between turbulence theory and experimental results convincingly suggest that the trapped electron modes dominate electron transport at low and moderate collisionality, when electron heating dominates. The threshold for these modes agrees with the experimental values. The stabilisation of these modes at high collisionality, as predicted by theory, is found in the experiments. Electron transport is then driven by the ion temperature gradient modes. At low collisionality, if trapped electron modes are stabilised by negative shear and shafranov shift effects, electron internal transport barriers may develop. This topic is also briefly addressed.

1. INTRODUCTION

In burning plasmas, the centrally peaked heating power provided by the Alpha particles will mainly be transfered to the electrons, whereas a large fraction of the ion heating will occur by electron-ion collisional transfer as energy flows towards the edge. Then, although fusion power is produced by a reaction between ions, electron heat transport is a key component in fusion processes in magnetically confined plasmas. It is therefore essential to gain a better physics understanding of the phenomena involved in electron transport, providing eventually reliable predictions for future devices. This is particularly important for electron heat transport which is larger by 2 or 3 orders of magnitude than diffusion due to collisions predicted by neoclassical theory. There is a large consensus to attribute this effect to turbulent transport driven by micro-instabilities.

On the experimental side, since the end of the 70's, electron temperature profiles in tokamaks have been observed to react weakly to changes of the heating power deposition profiles, a property named profile resilience or stiffness. An intense and coordinated effort, including common dedicated experiments, has been conducted during the last years to understand electron transport. It has been supported by the installation of systems for electron heating and measurement of the electron temperature. Several recent experimental results strongly suggest that profile stffness is most likely due to the existence of a threshold above which transport increases, in agreement with theoretical prediction for turbulent transport. In this paper we review the main experimental studies carried out on this subject during about the last 5 years. Emphasis is put on the tokamaks, but on some points a comparison with helical devices has been carried out for this work. This work deals with electron heat transport in the plasma core and does not include the edge in which the relevant physics may be quite different. Possible heat transport caused by MHD instabilities is not treated either.

In the next section the main theoretical elements are reviewed. Sections 3 and 4 are dedicated to experimental results on electron heat transport in conventional scenarios, whereas transport properties in plasmas with Internal Transport Barriers are addressed briefly in section 5.

2. ELEMENTS OF TURBULENT TRANSPORT THEORY

Theory of electrostatic turbulence indicates that electron heat transport in the plasma core may be driven by three electrostatic instabilities [1, 2, 3, 4]. This is valid if the ratio of plasma pressure to magnetic pressure (β) is low enough such that electromagnetic effects can be ignored. In the long wave length range (perpendicular scale 1=k_θ of the order of the ion Larmor radius ρ_i) the Trapped Electron Modes (TEM) [5, 6] and/or Ion Temperature Gradient (ITG) modes are most probable candidates. As will be shown later, the TEM instability is the main candidate to explain electron heat transport when electron heating is dominant. The ITG turbulence is well-known for its essential contribution to ion transport [7], but it also contributes, to a lesser extent, to electron heat transport [8]. In the short wave length domain, ($1/k_\theta \approx \rho_e$) the Electron Temperature Gradient (ETG) instability may exist [9], but can only drive a relevant flux if this turbulence develops larger radial cells, still a controversial topic. The most complete theoretical approach to characterize instabilities in the plasma core is provided by gyro-kinetic calculations, see e.g. [10]. The instabilities ITG, TEM and ETG have respective thresholds in ion or electron normalised temperature gradients, above which turbulence and the corresponding transport increase [2]. Formulae which can be easily compared with the experiment have been derived from linear gyro-kinetic calculations for the threshold of ETG [9] and TEM [11], the former also roughly applicable to ITG by reversing the role of the species. These are:

$$R/L_{Te}^{ETG} = (1 + Z_{eff}\, T_e/T_i)(1.3 + 1.91\hat{s}/q)(1 - 1.5\epsilon)[1 + 0.3(\kappa - 1)] \qquad (1)$$

$$R/L_{Te}^{TEM} = \frac{(0.357\sqrt{\epsilon} + 0.271)}{\sqrt{\epsilon}}\ [4.90 - 1.31\ \frac{R}{L_n} + 2.68\hat{s} + ln(1 + 20n_{eff})] \qquad (2)$$

Several plasma parameters play a role, local inverse aspect ratio ϵ = r/R, normalised density gradient R/L_n, effective charge Z_{eff}, temperature ratio T_e/T_i, magnetic shear s, safety factor q and plasma elongation κ. The ranges of validity are indicated in the respective publications. It should be underlined that they are not valid for $\hat{s} < 0.5$, a region where the threshold increases. The TEM instability being driven by trapped electrons the threshold decreases with increasing ϵ and, due to collisional detrapping, increases with collisionality characterized by $\nu_{eff} \propto \nu_{ei} / \omega D_e \approx 0.1R(Z_{eff}n_e)/T^2_e$ [12].

An empirical transport model based on the existence of a threshold $R/L_{Te,\,crit}$ has been successfully tested for ASDEX Upgrade ECRH heated plasmas [13] and applied later, in a generalized version, to also compare electron heat transport in different tokamaks [14]. It is written as:

$$\chi_e = \chi_s q^{3/2} \frac{T_e}{eB}\ \frac{\rho_s}{R}\left[\ \frac{R}{L_{Te}} - \frac{R}{L_{Te,\,crit}}\ \right]^{\alpha} H\left(\ \frac{R}{L_{Te}} - \frac{R}{L_{Te,\,crit}}\ \right) + \chi_0\ \frac{T_e}{eB}\ \frac{\rho_s}{R} \qquad (3)$$

It includes the increase of transport above the threshold $R/L_{Te,\,crit}$, through the Heaviside function H, as well as the gyro-Bohm factor $f_{gB} = (T_e/eB)(\rho_s/R) \propto T^{3/2}$. The dependence $q^{3/2}$ yields the required

radial dependence of transport as well as its dependence with plasma current [15]. Physically, this reflects the influence of the shift of the κ spectrum of the modes to lower values [16], specifically investigated for the TEM in gyro-kinetic non-linear calculations [17]. The non-dimensional coefficients χ_s, $R=L_{Te,\,crit}$ and χ_0 are adjusted such that the model reproduces the experimental results as well as possible. The rate of transport increase above the threshold is determined by the factor in front of the bracket, proportional to $\chi_s q^{3/2} T_e^{3/2}$. This determines the effective stiffness of the T_e profiles, in which $T_e^{3/2}$ plays an important role, whereas χ_s can be considered as an intrinsic stiffness. Consequently, for plasmas with high effective stiffness, in particular those at high temperature, the T_e profiles are closer to the threshold than those with low stiffness for which R/L_{Te} can exceed the threshold by a factor of 2 to 3 in present day tokamaks. The non-dimensional quantity χ_s allows for comparisons between different plasmas in various devices. For evaluating transport changes a normalisation by the gyro-Bohm factor and possibly $q^{3/2}$ is required. Finally, the exponent α has generally been set to unity, defining a linear increase of χ_e above the threshold. Recent gyro-kinetic results, [11, 10] yield a linear increase of the heat flux q_e above the threshold, which would rather correspond to a ≈ 0.5.

The properties of the empirical model have been discussed in details in [14]. In particular, the region around the plasma axis is always below the threshold, with a radial extension which depends on the experimental conditions and on the physics of transport. It should be also stressed that the edge temperature plays an important role.

3. EXPERIMENTAL APPROACH AND RESULTS IN CONVENTIONAL SCENARIOS

The clearest and simplest conditions to investigate electron heat transport are provided by plasma dominated by electron heating, generally at low density to reduce the coupling between electron and ion channels. The Electron Cyclotron Resonance Heating (ECRH) is the most suitable tool for such studies, because its power deposition occurs only on the electrons, in general in a narrow layer and is steerable by adjusting the mirror launchers and magnetic field value. For the second harmonic X-mode scheme, often used, the ECRH single pass absorption is generally 100%, allowing very clean experiments. Transport studies include power balance as well as investigation of transients excited by power modulation. The combination of the two approaches yields a rich and exigent set of information to constrain the models and better understand transport. The power balance analysis yields the usual electron heat diffusivity $\chi_e^{PB} = -q_e/(n_e \nabla T_e)$. The perturbative diffusivity deduced from heat pulse propagation yields $\chi_e^{HP} = \partial q_e/\partial(n_e \nabla T_e)$ and reflects the stiffness properties. It is also written as:

$$\chi_e^{HP} = \chi_e + \frac{\partial \chi_e}{\partial (T_e)} \quad T_{e,\,0} \tag{4}$$

which shows that χ_e^{HP} is in general larger than χ_e. The expression of χ_e^{HP} for the empirical model can be easily derived from Eq.3:

$$\chi_e^{HP} = \chi_s q^{3/2} \frac{T_e}{eB} \frac{\rho_s}{R} \left[2\frac{R}{L_{Te}} - \frac{R}{L_{Te,\,crit}} \right] H \left(\frac{R}{L_{Te}} - \frac{R}{L_{Te,\,crit}} \right) + \chi_0 \frac{T_e}{eB} \frac{\rho_s}{R} \quad (5)$$

Experimentally, the quantity χ_e^{HP} is deduced from the analysis of the T_e modulation data by well-known methods [18, 19]. Fourier analysis of T_e yields amplitude and phase profiles of the perturbation from which one deduces respectively χ_e^{Amp} and χ_e^{phi} which yield $\chi_e^{HP} = \sqrt{\chi_e^{Amp}\,\chi_e^{phi}}$. Power modulation for transport studies is applied with frequencies ranging from about 10Hz to a few hundred Hz, depending on the conditions and on machine size. The measurement of T_e by Electron Cyclotron Emission (ECE) heterodyne radiometers, available on most of the fusion devices, fulfills the requirements: the time resolution reaches easily several kHz, the number of channels (up to 100) is largely sufficient and the spatial resolution per channel very good. Therefore the combination of ECE and ECRH provides the best conditions for electron heat transport studies. In JET, for which ECRH is unfortunately not available, electron heating with ICRF in mode conversion scheme has proven useful [20].

3.1. OVERVIEW OF THE RESULTS AND DEVICE COMPARISONS

Numerous experiments show that the electron (and ion) temperature profiles react weakly to changes of the heating power deposition [21, 22, 23, 24, 25, 26, 27, 28, 29, 30]. In particular, the quantity R/L_{Te} remains clearly positive in most of the cases, even with strong off-axis heating. A significant variation of the radial distribution of the power deposition profile is needed to vary R/L_{Te}, for instance on-axis or off-axis heating. This can be, in particular, provided by two ECRH beams depositing their power centrally, P_{ECin}, and off-axis, P_{ECout}, at typical radial positions $\rho_{in} \approx 0.3$ and $\rho_{out} \approx 0.7$, ρ being a normalised radius. In addition, one can vary the ratio P_{ECin} / P_{ECout} while keeping $P_{ECin} + P_{ECout}$ constant, ensuring a constant edge temperature and small variations of T_e between the two depositions where the analysis is then carried out. Such experiments, in L-mode, have been performed initially in ASDEX Upgrade (AUG) [15] and repeated in DIII-D [31] and TCV [32]. In addition, in AUG and DIII-D power modulation was applied yielding χ_e^{HP}. In the TCV tokamak, the flexible plasma shaping capabilities have been used to test the influence of plasma triangularity (δ) on transport, including strongly negative δ values, [32, 33]. The results indicate that electron heat transport, in such L-mode TEM dominated plasmas, decreases by about a factor of 2 from $\delta = +0.4$.

The results from AUG and DIII-D agree well, Fig.1 left plot. The power balance data clearly point toward a finite value of R/L_{Te} for zero transport. The χ_e^{HP} and χ_e^{PB} data are compatible with the hypothesis described by Eq.3 and 5 as shown by the lines which are provided by the model with the parameters indicated in the caption. The lines indicate the jump-like behaviour of χ_e^{HP} at the threshold which is a good experimental monitor for the existence of a threshold. The difference in $R/L_{Te,\,crit}$ is within the experimental uncertainties. The value for χ_s in this analysis at $\rho \approx 0.5$ is rather similar. However, the full transport simulations with the empirical model require somewhat larger differences in χ_s (0.2 for AUG, 0.4 for DIII-D) to obtain an acceptable agreement with the experimental T_e profiles over the whole radius. This difference in χ_s, which is larger than expected

for devices and plasmas which are so similar, is still under investigation. In the right plot of Fig.1 we show the normalised heat flux and diffusivity versus R/L_{Te} in the experiments carried out in TCV. Note that, thanks to the large power density available in TCV, the range explored in R/L_{Te}, up to 20, is about a factor of 2 larger than in AUG and DIII-D. Here also, q_e unambiguously points toward a finite value of R/L_{Te} for zero heat flux. Its behaviour is initially almost linear and suggest a saturation at higher values of R/L_{Te}. This leads to the strong saturation of χ_e for $R/L_{Te} \geq 10$. In ASDEX Upgrade, the transport properties exhibited by such experiments have been compared in detail with linear gyro-kinetic calculations [11]. They indicate that the TEM instability dominates electron heat transport under such conditions. The threshold and the rate of transport increase above it agree very well. On the other hand, theory predicts the TEM driven heat flux to be linear in R=LTe sufficiently above the threshold [11, 10]. This appears to be supported by the TCV data whereas this could not be verified in the other devices ($R/L_{Te} < 10$) within the experimental uncertainties. However, it should be noted that varying the ECRH deposition from off-axis to on-axis leads to an increase of s, and therefore of R/L_{Te}^{TEM}, which might influence the experimental dependence of $q_e = f(R/L_{Te})$. Thus, the empirical model, linear in χ_e($\alpha = 1$ in Eq.3) and corresponding to $q_e \propto (R/L_{Te})^2$, gives good results in the devices for which the excursion in R/L_{Te} remains below 10 where one cannot distinguish between linear and quadratic behaviors within the uncertainties. It must be underlined that in these AUG and DIII-D experiments, even in the pure off- axis case, the value of R/L_{Te} remained most probably (just) above the threshold. Indeed, transport becomes very low when approaching the threshold and the residual Ohmic heat flux was high enough to prevent the Te profile from dropping below the threshold. Therefore, these results strongly suggest the existence of a threshold in R/L_{Te}, but could not actually prove its existence without ambiguity, leaving room for other interpretations [31]. We will show in the next subsection that operating at lower plasma current allows one to force the profiles below threshold with off-axis heating. Other indications of the existence of a threshold were reported in Tore Supra [34, 35], FTU [36, 37] and JET [20]. From the analysis of Tore Supra data, a formula for the experimental threshold with a dependence on $\hat{s}/q$ has been deduced, but the type of unstable modes were not be determined without ambiguity, ETG are also possible candidates [35]. For DIII-D, a detailed study of the effect of perturbations by sawteeth and modulated ECRH in the (q_e, ∇T_e) plane has been reported in [38]. The patterns are compatible with the empirical model. In DIII-D [31] and TCV [39], local modulation of the temperature gradient and magnetic shear with ECRH/ECCD have been carried out respectively. The latter exhibits a relation between shear and transport. In ASDEX Upgrade, the time evolution of the T_e profile after the turn-on and turn-off of ECRH has been shown to be in rather good agreement with the empirical model [40].

The existence of a threshold close to which transport is small together with the presence of the residual Ohmic heat flux in tokamaks contribute strongly to the weak reaction of the T_e profiles to changes of heating deposition profiles, known as resilience or stiffness. It should be stressed that the dependence of the edge temperature on heat flux play a major role. It must be stressed that the

experiments with on-axis and off-axis heating demonstrate that rather large variations of R/L_{Te} above the threshold are possible in present experiments. The values found for χ_s in pure electron heating and which can be attributed to TEM transport are smaller by about a factor of 10 compared to what is expected for ion transport driven by ITG [14]. The T_e profiles determined by TEM- driven transport should be considered as weakly stiff.

As already mentioned above, the empirical model has been successfully used for comparisons between devices, AUG, JET, FTU and Tore Supra, [14, 41]. The values of χ_s for dominant electron heating are in the range is 0.2 - 0.5. The values found for the threshold in the multi-machine study also cover a wide range: $3 \leq R/L_{Te,\ crit} \leq 8$. The formula for the TEM given in [11] provides a possibility to investigate the reasons of this range, as shown in Fig.2. As mentioned in [11], the threshold given by the formula is obtained from a linear extrapolation to zero flux and the actual threshold is lower by a factor 0.9 to 0.65 depending on R/L_n. This correction has been applied here, taking into account the results shown in Fig.3 of Ref. [11]. The left plot of Fig.2 shows this corrected TEM threshold versus the threshold values yielded by the simulations with the empirical model in the different devices. There is a clear relationship. The variation of R/L_{Te}^{TEM} is dûe to the ranges in R/L_n, s and ν_{eff} which vary signficantly, as shown in the right plot of Fig.2. For FTU the value of $R/L_{Te,\ crit}$ represents a typical number for several discharges without modulation. It is therefore determined with less accuracy than for the other devices. The results of Fig.2 are an additional confirmation of the usefulness of the empirical model and also a useful experimental validation of the TEM formula.

The major electron transport issue of low-shear stellarators are the neoclassical transport physics in the plasma core with the development of the neoclassical electron root for collisionalities [42] and the strong variation of confinement with rotational transform [43] Encouraged by this coherent picture in tokamaks, data from the W7-AS stellarator (shut down since 2002) have been analysed as proposed in this paper. This approach is justified by the gyro-Bohm dependence found in W7-AS for the electrons [44], by the similarities of confinement between tokamaks and stellarators [45, 46] and by the measurement of fluctuations in the plasma core [45]. The plasmas chosen for the study presented here were heated by a combination of on-axis and off-axis ECRH, see [46] Fig.25. For the on-axis cases the ECRH powers were 0.1, 0.4 and 0.8MW. For the off-axis cases, 0.4MW were applied at $\rho \approx 0.6$ combined with either 0.1, 0.2 or 0.4MW of central heating. In these experiments, the total heating power was varied between 0.1MW and 0.8MW from case to case, leading to a large variation of T_e and the gyro-Bohm normalisation is essential. The results from the analysis carried out between the 2 depositions, at $\rho \approx 0.4$, are given in Fig.3.

The left plot shows, here also, that the normalised heat diffusivity points toward a finite value of $R/L_{Te} \approx 15$. Numerical simulations with the empirical model agree well with the data, as shown by the open dots in this plot and also by the T_e and χ_e profiles for two of the cases illustrated in the right plot. The simulations require $\chi_s = 0.2$, well in the range of ECRH heated plasmas in tokamaks. Therefore the T_e profiles are also not highly resilient and due to the relatively low temperature the

effective stiffness is low. The point with the highest value of R/L_{Te} is from the discharge with a total heating power of only 0.1MW deposited in the center. It has a very low temperature $T_e(\rho = 0.5) \approx$ 0.15keV and the high values of $q_e/T_e^{5/2}$ and R/L_{Te} are due to this. Modeling this point requires taking into account edge radiation to keep T_e low enough in the outer region $\rho > 0.8$ and the result for this point is uncertain. The value for the threshold ≈ 15 is large compare to those found in tokamaks. Under the assumption of TEM driven transport, this is explained qualitatively by the large aspect ratio of the device, the specific trapping configuration for electrons and by the at shear. On the other hand, ETG modes may be active in W7-AS and a threshold formula for this device, [47], yields in this case $R/L_{TETG} \approx 13$ compatible with the experimental value. On that basis, it is not possible to make any statement on the type of turbulence, but the existence of a threshold seems plausible.

The absence of Ohmic heating in stellarators makes a decisive difference for the T_e profile behaviour compared to that in tokamaks: for purely off-axis ECRH, the central heating source is rigorously zero and the T_e profiles cannot be sustained above the threshold, always leading to hollow profiles, see e.g. [48]. Therefore, this apparent contradiction between tokamaks and stellarators may be understood in the frame of the model. An argument against the hypothesis of such a type of transport has been that modulation experiments yielded $\chi_e^{HP} \approx \chi_e^{PB}$ in W7-AS, [45]. From the model, one would expect $\chi_e^{HP} \approx 3\chi_e^{PB}$. More recent data suggest that $\chi_e^{HP} > \chi_e^{PB}$ increases above unity as the total heating power is increased to decrease towards unity if power is further increased [49]. This might be in closer agreement with a linear dependence of heat flux on R/L_{Te}, as discussed in [11]. Finally, the data analysed for the present paper are only a small subset of data from transport studies in W7-AS in which a large variety of shapes for the T_e profile can be obtained [50]. Further comparisons with the hypothesis of a threshold in R/L_{Te} would be very instructive but it was out of the possibilities for this paper.

The results presented above were deduced from discharges in tokamaks and helical devices with strong electron heating and $T_e > T_i$ in which TEM dominate electron heat transport, the ITG contribution is small due to the low ion heat flux, TEM and ITG are not strongly coupled. In plasmas with comparable electron and ion heating, $T_e \leq T_i$, typically NBI heated L and H modes, the situation is quite different. The three instabilities, TEM, ITG and ETG, can coexist leading to a very complicated situation. In addition, the experimental possibilities to vary R/L_{Te} are limited because, even with strong off-axis ECRH, the electron heat flux due to the NBI heating is not negligible. Approaching or crossing a possible threshold can be achieved at radial positions which are close enough to the plasma axis, as indicated above. This has been observed experimentally, but this is not always possible because often dominated by the sawtooth activity. Dedicated experiments with modulated ECRH have been carried out in DIII- D L-modes [51] and ASDEX Upgrade H-modes [52]. None of these studies provided definitive results on the type of transport, those in ASDEX Upgrade might suggest a threshold in the central region at $\rho \approx 0.2$ and a transition in transport properties at $\rho \approx 0.45$. Experiments in JET L and H modes with modulated ICRF mode conversion could be modeled satisfactorily with the empirical model [20], the values of s reaching up to about 1, [14].

They suggest a trend for χ_s to increase with the fraction of ion heating, also found in simulations with fluid models [20].

3.2. EXPERIMENTAL EVIDENCE FOR THE R=LTE THRESHOLD

The tokamak experiments described above strongly suggest the existence of a threshold, but could not show it explicitly because the residual Ohmic power prevented the profile from dropping below the threshold, even with off-axis heating. Therefore, similar experiments have been repeated in ASDEX Upgrade at lower plasma current in which R/L_{Te} could be varied across the threshold [53]. The results are shown in Fig.4.

The left plot shows the dependence of the electron heat flux versus R/L_{Te} which clearly exhibits a change of slope at $R/L_{Te} \approx 3$, as expected for a threshold. The fact that q_e is low but positive below the threshold rules out the necessity of an inwardly directed heat pinch to explain the offset in R/L_{Te}. The values of P_{ECin}, indicated for each point in the plot, show that indeed very low power (below 90kW) is required to sustain the T_e profile just above the threshold. In these discharges P_{ECout} was modulated with an amplitude of about 10%. The right plot shows the resulting heat pulse diffusivities χ_e^{amp} and χ_e^{phi} deduced from the amplitude and the phase of the modulated T_e, using the usual method [18]. They also exhibit a clear jump-like behaviour at $R/L_{Te} \approx 3$ which corresponds to what is expected for a threshold. Here, we find $\chi_a^{amp} > \chi_e^{phi}$ which is not usual, in general $\chi_a^{amp} \leq \chi_e^{phi}$ due to damping effects [54]. The situation found here is caused by a distortion of the amplitude and phase profiles induced by a secondary wave excited at the deposition of P_{ECin}. In fact, the incoming pulses cause a cyclic variation of R/L_{Te} which induces a modulation of χ_e. In the region where P_{ECin} is deposited, this is equivalent to a modulated heat source there, [55, 56], and therefore excites a secondary wave which interferes with the incoming one launched by P_{ECout}. Even if the amplitude of the secondary wave is small, this interference can significantly distort the amplitude and phase profiles with respect to the situation without this effect. This strongly influences χ_e^{Amp} and χ_e^{phi} which depend on the respective profile slopes squared.

4. TYPE OF TURBULENCE, TRANSITION FROM TEM TO ITG

In ASDEX Upgrade[11], DIII-D[31], JET (done for this work) and TCV [32] gyro- kinetic stability calculations indicate that with $T_e > T_i$ and at moderate values of collisionality, typically $\nu_{eff} < 1$, the turbulence excited by the TEM dominates electron heat transport. However, if collisionality is increased, the TEM is gradually stabilised and the dominant mode is found to be the ITG [53, 32]. In fact, the ITG modes, well-known for their contribution to ion heat transport, also drive some electron heat flux. In the cases where the TEM is stable, this becomes a crucial ingredient of electron heat transport. In TCV, a decrease of transport is measured as eff increases, Fig.5 left plot, and the lowest normalised diffusivities are dominated by ITG, [32].

In ASDEX Upgrade modulation experiments in a collisionality scan, $0.3 < \nu_{eff} < 6$, [53], exhibit a sharp and strong drop of χ_e^{HP}/χ_e^{PB} at $\nu_{eff} \approx 2$, Fig.5 right plot. The unusual situation $\chi_e^{HP}/\chi_e^{PB} < 1$

reflects a very weak dependence of q_e versus ∇T_e. It is interpreted as a transition from TEM to ITG dominated heat transport and explained by the different dependence versus R/L_{Te} of the electron heat flux driven by TEM or ITG [53]. Whereas the heat flux driven by the TEM increases continuously with R/L_{Te}, that driven by ITG saturates at $R/L_{Te} \approx 10$ yielding very low values of χ_eHP.

The TEM-ITG transition also plays an important role in the behavior of the density profiles because it influences the direction of the particle pinch, inwards for ITG, outwards for TEM, [57]. In particular, the 'pump out' effect caused by ECRH in some cases is explained by a transition to TEM-driven transport with more electron heating [58]. Such observations are coherent with the results presented in this section.

5. TRANSPORT IN ELECTRON ITBS

Internal Transport Barriers characterized by large temperature and pressure gradients are able to yield simultaneously a substantial fraction of non-inductive bootstrap current and high performance due to the high temperature which can be reached. Scenarios exploiting the dominant ion heating by NBI have been extensively investigated [59, 60]. They produce strong ITBs in the ion channels but generally weak or no ITBs in the electron channels. The physics of ITBs has been very comprehensively reviewed in [59] and we focus here only on very recent results on electron ITBs. Strong electron ITBs have been created with dominant electron heating, generally in conjunction with current drive, using RF scenarios such as LH, ECH and ICRF. Pure electron ITBs are not envisaged as a scenario for future burning plasmas but provide interesting plasmas which complement the transport and ITB studies. The main experimental studies and results on eITBs have been reviewed in [61] and can be found for the different tokamaks as follows: ASDEX Upgrade [62, 63]; DIII-D [64]; FTU [65, 66], JET [67, 68]; JT-60U [69, 70]; Tore Supra [71, 72]; TCV [73, 74, 75]; T-10 [76, 77]. Electrons ITBs, generally obtained at very low densities, with cold ions, lead to central electron temperatures which can reach up to 20keV. Power balance analyses indicate that the electron heat diffusivity χ_e drops by almost an order of magnitude across an electron ITB. Typical values are 1 to 4 m^2/s outside of the barrier and 0.5 to 0.1 m^2/s inside of the barrier, see for instance [65, 67, 72, 78]. The latter value is low but remains above the electron neoclassical value. Therefore turbulent transport is no fully suppressed, in contrast to what is observed in ion ITBs. The creation of an electron ITB is clearly linked with a change of q profile and requires in general a shear profile with a local minimum, i.e. a central region with negative shear [76, 77, 68, 70, 79, 74, 75, 66]. As indicated above, one expects TEM driven turbulence being responsible for electron heat transport in most of the low density plasmas heated with pure electron heating before the eITB formation. Indeed, the analyses indicate that the stabilisation of these modes causes the eITB [80, 68, 81]. In general, the radial position of the barrier foot is related to the position of the minimum q value, however, due to the uncertainties of that quantity it is not possible to specify if it is right at this position. The stabilisation is found to be due to the negative shear in conjunction with the Shafranov shift, the latter being essential, whereas the velocity shearing plays a minor

role in eITBs [80, 81].

Electron ITBs have also been created and investigated in several helical devices as reported in the very recent and complete review, [50] and references therein, to which we refer the reader. It should be underlined that the mechanism for the eITB formation in helical devices differs from what happens in tokamaks. It is due to the transition to the electron root of transport, occurring at low collisionality and correlated with a high positive radial electric field.

For the experimental results in tokamaks, we illustrate here two main lines of experimental studies for eITBs: (i) the relation between q profile and barrier properties; (ii) the evidence of a barrier via transient transport methods. In ASDEX Upgrade, JT60- U and TCV the strength of the barrier, for instance characterized by R/L_{Te}, has been shown to increase with the amount of ctr-ECCD driven on the plasma axis [82, 78, 70].

In TCV, thanks to the powerful ECRH/ECCD capabilities and to the short current diffusion time, steady-state eITBs could be sustained in fully non-inductive plasmas (zero loop voltage) the current being driven by ECCD and bootstrap current [83]. This property has been used in recent experiments in which a ne dosing of additional Ohmic current has been applied in such discharges with eITB to vary the q profile. This clearly demonstrates the relation between barrier strength and negative shear [74, 75] and Fig. 6.

The relationship between shear and transport in the eITB formation has been observed dynamically in Tore Supra in the so-called giant oscillations [84]. This phenomenon, in which an eITB develops and then disappears during a cycle evolution of the current profile, leads to excursions in the central T_e of several keV. The mechanisms underlying the giant oscillations are likely linked to the negative magnetic shear in the vicinity of a low order rational surface ($q = 2$) and a possible action of the (2,1) tearing mode. These results yields information on the dynamics of eITBs.

Attempts to diagnose eITBs using transient transport have been carried out with cold pulses in JET [85] and JT60-U [86, 87], as well as with ICRF power modulation in JET [88]. These experiments exhibit a decrease of the propagation speed of the perturbation when crossing the barrier. An example is shown in Fig.7 for the JET experiment with modulated ICRF in the ^{3}He mode conversion scheme for electron heating. In this case, the same ICRF wave deposits its power at 2 positions (FW and MC) and both are therefore modulated. This complicates the heat pulse propagation pattern as the two heat waves interfere. However Fig.7 indicates that in the presence of the ITB the heat waves exhibit a strong decrease of the propagation speed in the region of the barrier, as shown by the change of slope of the amplitude and phase profiles in this region. This effect is not visible in the absence of ITB.

CONCLUSIONS AND DISCUSSION

Numerous and detailed experimental studies of electron heat transport have been carried out in various devices. Most of them are provided by the extremely fruitful combination of flexible ECRH heating systems and ECE measurement of T_e. Power balance and heat pulse analyses yield a very

complete picture of the transport properties. The experimental results agree with the predictions of turbulent transport theory, as shown by several direct comparisons. In the plasmas with electron heating and $T_e > T_i$ at moderate collisionality, the TEM instability is shown to dominate electron heat transport. Theory predicts a threshold which has indeed been found in the experiments. Moreover, the expected stabilisation of the TEM by collisions has also been observed, leading to a TEM-ITG transition in the electron channel.

An inwardly directed anomalous heat pinch has been often advocated to explain the resilience of T_e profiles in tokamaks. The results presented here strongly suggest that this effect is not required: a finite threshold in R/L_{Te} and the residual Ohmic flux are found to be sufficient in most of the cases. Experiments with off-axis ECRH modulated at low frequency were thought to be able to demonstrate the existence of a pinch by a distortion of the amplitude profile. Indeed, studies carried out in ASDEX Upgrade exhibit a distortion of the amplitude, which, however, is compatible with the empirical model with threshold [89]. This is due to the modulation of the T_e profiles back and forth around the threshold and by an apparent convective term reflected in the modulation data due to the temperature dependence, as pointed out in [13]. However, a small heat pinch cannot be excluded to ensure $\chi_e^{PB} \geq 0$, but its values is too small to explain the distortion of the amplitude profile.

Very fast transients in electron heat transport are observed in some cases, for instance the propagation of cold pulses in TEXT [90] and JET [85], with or without polarity in- version, or temperature changes at the ECRH turn-on or turn-o in W7-AS [91]. Such effects, considered as an indication for non-local transport, are not reproduced by the physics described above, suggesting that more elements may play a role under specific conditions.

In burning plasmas, such as expected in ITER, electron heating will dominate and $T_e > T_i$ is expected over a significant radial region of the plasma. As collisionality will be lower than in present experiments, one may expect TEM-driven transport to play a role. A quantitative assessment of TEM-driven transport can be probably deduced from comparisons between results such as those presented above and non-linear gyro-kinetic calculations. This should be a possible task for the near future.

For plasmas with equivalent electron and ion heating, which will exist in burning plasmas outside of the very center, the situation is more complex, the different instabilities (TEM, ITG and ETG) may be all active. Clearly, the physics understanding in this regime should be improved, this can be done in present devices and further intensive studies are required. They should probably combine dedicated transport investigations, turbulence measurements and comparisons with non-linear gyro-kinetic calculations. Moreover, in such conditions, the different transport channels cannot be separated and taking into account particle and heat transport in a combined way will be required. In ITER, due to the high temperatures, profiles will have a higher effective stiffness and be much closer to the thresholds than at present. Therefore not only transport should be assessed quantitatively as well as possible, but also the thresholds. In addition, the edge (or pedestal) temperature is a key parameter in the determination of the temperature profile. Its prediction is still an important issue

in the frame of electron heat transport for future devices.

ACKNOWLEDGMENT

It is a pleasure to acknowledge the indispensable support of the technical staff of the devices and heating systems as well as the precious contribution of the colleagues in charge of the diagnostics. The first author is deeply grateful to C. Angioni and A.G. Peeters for their patient and numerous explanations on transport theory. We also thank the colleagues who provided us with published material used in this paper. The work on DIII-D was partially supported by the US DOE under GA-DE-FC02-04ER54698.

REFERENCES

[1]. W. Horton, Rev. Mod. Phys. **3** (1999) 735.
[2]. X. Garbet, Plasma Phys. Controlled Fusion **43** (2001) A251.
[3]. B. Scott, This issue (2006).
[4]. A. G. Peeters, This issue (2006).
[5]. H. Nordman et al., Nucl. Fusion **30** (1990) 983.
[6]. J. Weiland, Collective Modes in Inhomogeneous Plasmas, IOP Publ. , Bristol, 2000.
[7]. A. Dimits et al., Phys. Plasmas **7** (2000) 969.
[8]. M. A. Beer et al., Phys. Plasmas **3** (1996) 4018.
[9]. F. Jenko et al., Phys. Plasmas **8** (2001) 4096.
[10]. F. Jenko et al., Plasma Phys. Controlled Fusion **47** (2005) B195.
[11]. A. G. Peeters et al., Phys. Plasmas **12** (2005) 022505.
[12]. C. Angioni et al., Phys. Plasmas **10** (2003) 3225.
[13]. F. Imbeaux et al., Plasma Phys. Controlled Fusion **43** (2001) 1503.
[14]. X. Garbet et al., Plasma Phys. Controlled Fusion **46** (2004) 1351, Addendum in Plasma Physics and Controlled Fusion **47**, 6, pp. 957{958 (2005).
[15]. F. Ryter et al., Nucl. Fusion **43** (2003) 1396.
[16]. R. E. Waltz et al., Phys. Plasmas **4** (1997) 2482 .
[17]. T. Dannert et al., Phys. Plasmas **12** (2005) 072309.
[18]. N. J. Lopes Cardozo, Plasma Phys. Controlled Fusion **37** (1995) 799.
[19]. A. Jacchia et al., Phys. Fluids B **3** (1991) 3033.
[20]. P. Mantica et al., 19th IAEA Fusion Energy Conference, Lyon, France, Paper EX/P1-04 (2002).
[21]. V. Alikaev et al., Plasma Phys. Contr. Fus. Res., Proc. 11th IAEA Conf., Kyoto, 1986, **3** (1987) 111.
[22]. F. Wagner et al., Phys. Rev. Lett. **56** (1986) 2187.
[23]. G. Taylor et al., Nucl. Fusion **29** (1989) 3.
[24]. T. C. Luce et al., Phys. Rev. Lett. **68** (1992) 52.

[25]. M. Greenwald et al., Nucl. Fusion **37** (1997) 793.
[26]. W. Suttrop et al., Plasma Phys. Controlled Fusion **39** (1997) 2051.
[27]. P. Gohil et al., Nucl. Fusion **38** (1998) 425.
[28]. L. D. Horton et al., Plasma Phys. Controlled Fusion **41** (1999) B329.
[29]. F. Ryter et al., Plasma Phys. Controlled Fusion **43** (2001) A323.
[30]. H. Urano et al., Nucl. Fusion **42** (2002) 76 .
[31]. J. C. DeBoo et al., Nucl. Fusion **45** (2005) 494.
[32]. Y. Camenen et al., Plasma Phys. Controlled Fusion **47** (2005) 1971.
[33]. Y. Camenen et al., to be presented at 21st IAEA Fusion Energy Conference, Chengdu, China (2006).
[34]. G. T. Hoang et al., Phys. Rev. Lett. **87** (2001) 125001.
[35]. G. T. Hoang et al., Phys. Plasmas **10** (2003) 405.
[36]. A. Jacchia et al., Nucl. Fusion **42** (2002) 1116 .
[37]. S. Cirant et al., Nucl. Fusion **43** (2003) 1384 .
[38]. K. W. Gentle et al., Physics of Plasmas **13** (2006) 012311.
[39]. S. Cirant et al., Nucl. Fusion **46** (2006) 500.
[40]. K. K. Kirov et al., Plasma Phys. Controlled Fusion **48** (2006) 245.
[41]. X. Garbet et al., Plasma Phys. Controlled Fusion **46** (2004) B557.
[42]. H. Maassberg et al., Phys. Plasmas **7** (2000) 295.
[43]. R. Brakel et al., Nucl. Fusion **42** (2002) 903.
[44]. U. Stroth et al., Phys. Rev. Lett. **70** (1993) 936.
[45]. H. J. Hartfu et al., Plasma Phys. Controlled Fusion **36** (1994) B17.
[46]. U. Stroth, Plasma Phys. Controlled Fusion **40** (1998) 9.
[47]. F. Jenko et al., New Journal of Physics **4** (2002) 35.
[48]. V. Erckmann et al., Nucl. Fusion **43** (2003) 1313.
[49]. H. Walter, Strexperimente zur Untersuchung des Energietransports im Stellarator Wendelstein 7-AS, Doctoral thesis, Max-Planck-Institut für Plasmaphysik, Garching, Germany, 1998.
[50]. F. Wagner et al., Plasma Phys. Controlled Fusion **48** (2006) A217.
[51]. J. C. DeBoo et al., Nucl. Fusion **39** (1999) 1935.
[52]. A. Manini et al., Plasma Phys. Controlled Fusion **46** (2004) 1723.
[53]. F. Ryter et al., Phys. Rev. Lett. **95** (2005) 085001.
[54]. T. C. Luce et al., Proc. Workshop on Local Transport Studies in Fusion Plasmas (Varenna 1993), Bologna: Societa Italiana di Fisica (1994) 155.
[55]. U. Stroth et al., Local transport studies in fusion plasmas, ed. J.D. Callen et al. Bologna (1994) p. 161 .
[56]. A. Jacchia et al., Phys. Plasmas **2** (1995) 4589.
[57]. C. Angioni et al., Nucl. Fusion **44** (2004) 827.
[58]. C. Angioni et al., Phys. Plasmas **12** (2005) 040701.

[59]. J. Connor et al., Nucl. Fusion **44** (2004) R1.
[60]. X. Litaudon, Plasma Phys. Controlled Fusion **48** (2006) A1.
[61]. E. Barbato, Plasma Phys. Controlled Fusion **43** (2001) A287.
[62]. R. C. Wolf et al., Nucl. Fusion **41** (2001) 1259.
[63]. F. Leuterer et al., Nucl. Fusion **43** (2003) 1329.
[64]. C. M. Greenfield et al., in Europhysics Conference Abstracts (CD-ROM), Proc. of the 27th EPS Conference on Controlled Fusion and Plasma Physics, Budapest, 2000, edited by K. Szegö et al., volume 24B, pages 544{547, Geneva, 2000, EPS.
[65]. V. Pericoli Ridolfini et al., Nucl. Fusion **43** (2003) 469.
[66]. C. Sozzi et al., Journal of Physics: Conference Series **25** (2005) 198.
[67]. G. M. D. Hogeweij et al., Plasma Phys. Controlled Fusion **44** (2002) 1155.
[68]. Y. F. Baranov et al., Plasma Phys. Controlled Fusion **46** (2004) 1181.
[69]. S. Ide et al., Nucl. Fusion **44** (2004) 87.
[70]. T. Fujita et al., Plasma Phys. Controlled Fusion **46** (2004) A35.
[71]. G. Hoang et al., Nucl. Fusion **40** (2000) 913.
[72]. X. Litaudon et al., Plasma Phys. Controlled Fusion **43** (2001) 677.
[73]. M. A. Henderson et al., Plasma Phys. Controlled Fusion **46** (2004) A275.
[74]. O. Sauter et al., Phys. Rev. Lett. **94** (2005) 105002.
[75]. T. P. Goodman et al., Plasma Phys. Controlled Fusion **47** (2005) B107.
[76]. K. A. Razumova et al., Plasma Phys. Controlled Fusion **45** (2003) 1247.
[77]. N. A. Kirneva et al., Plasma Phys. Controlled Fusion **47** (2005) 1787.
[78]. Z. A. Pietrzyk et al., Phys. Rev. Lett. **86** (2001) 1530.
[79]. M. A. Henderson et al., Phys. Rev. Lett. **93** (2004) 215001.
[80]. A. G. Peeters et al., in Proc. of the 18th IAEA Conference Fusion Energy (CD-Rom), Sorrento, Italy, October 2000, volume IAEA-CSP-8/C, pages IAEA-CN-77/EXP5/06, Vienna, 2001, IAEA.
[81]. A. Bottino et al., Plasma Phys. Controlled Fusion **48** (2006) 215.
[82]. F. Leuterer et al., Nucl. Fusion **43** (2003) 744.
[83]. O. Sauter et al., Phys. Rev. Lett. **84** (2000) 3322.
[84]. F. Imbeaux et al., Phys. Rev. Lett. **96** (2006) 045004.
[85]. P. Mantica et al., Plasma Phys. Controlled Fusion **44** (2002) 2185.
[86]. S. Inagaki et al., Plasma Phys. Controlled Fusion **46** (2004) A71.
[87]. S. Inagaki et al., Nucl. Fusion **46** (2006) 133.
[88]. P. Mantica et al., Phys. Rev. Lett. **96** (2006) 095003.
[89]. P. Mantica et al., Plasma Phys. Controlled Fusion **48** (2006) 385.
[90]. K. Gentle et al., Phys. Plasmas **4** (1997) 3599.
[91]. U. Stroth et al., Plasma Phys. Controlled Fusion **38** (1996) 611, Corrigendum in Plasma Phys. Contr. Fus., 38 1087 (1996).

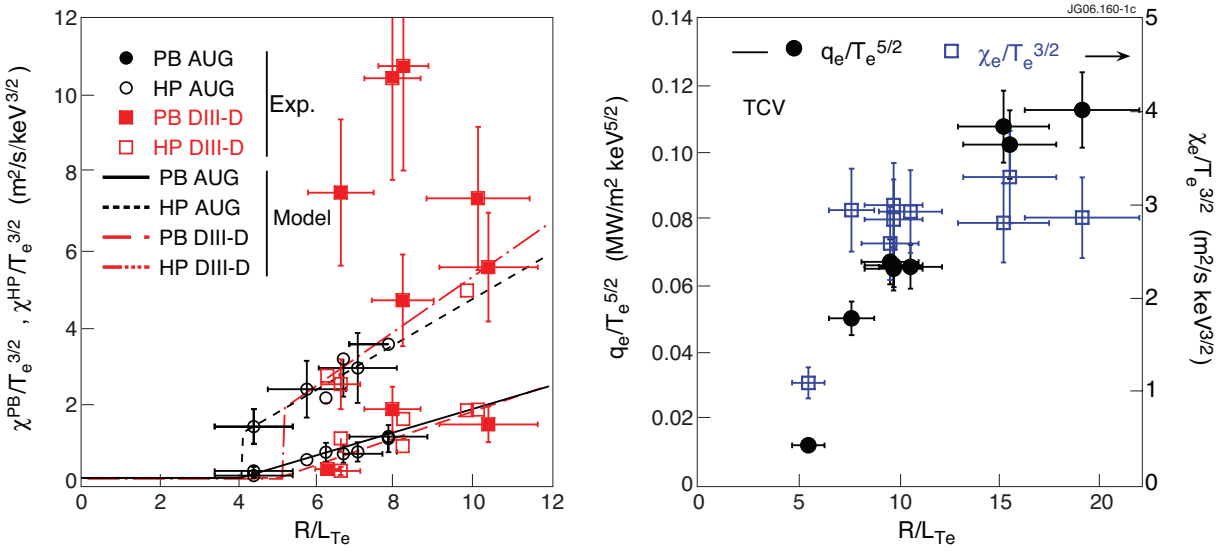

Figure 1: Left plot: AUG and DIII-D (adapted from [31]). Normalised power balance and heat pulse diffusivities versus R=L_{Te}, at ρ ≈ 0.5. Experimental data and simulations with the empirical model for which the parameters are: χ_s^{AUG} = 0.25 χ_s^{DIII-D} = 0.3, $R/L_{Te,\,crit}^{AUG}$ = 4, $R/L_{Te,\,crit}^{DIII-D}$ = 5. The 3 higher χ_e^{HP} points for DIII-D are not understood.
Right plot: TCV normalised electron heat ux and di usivity versus R=L_{Te} at ρ = 0.5, for the case δ = 0.2 (adapted from [32]).

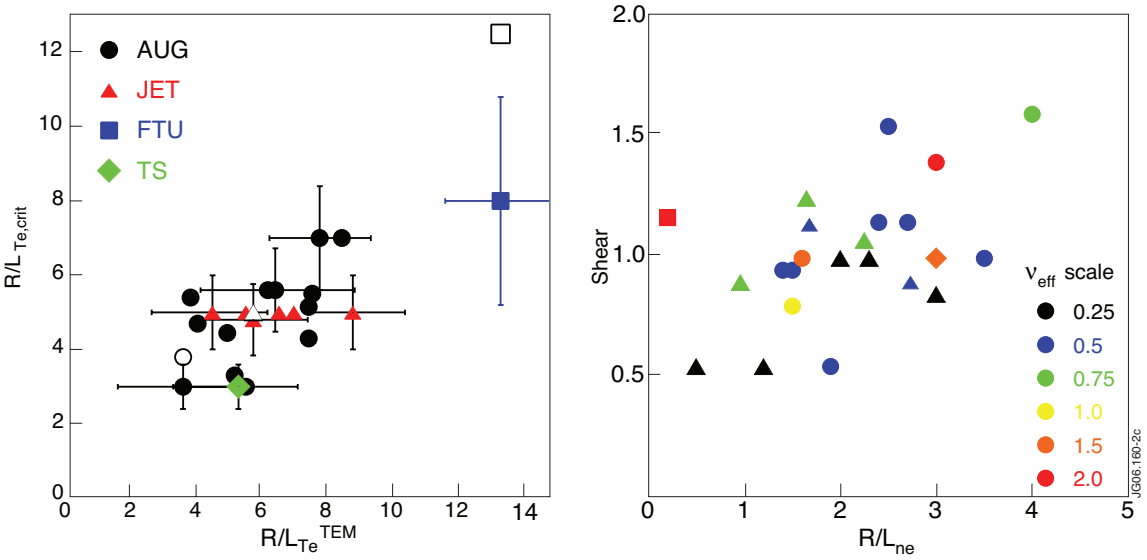

Figure 2: Left plot: Threshold yielded by simulation with the empirical model [14] in AUG,FTU,JET and TS versus TEM threshold from Eq.2. Open symbols indicate the threshold from gyro-kinetic calculations for speci c discharges, the correspondence is indicated by a segment linking this point to the corresponding full symbol.
Right plot: Ranges in R=L_n, ŝ and νeff (colour code) for the same data and same symbols shape as in the left plot.

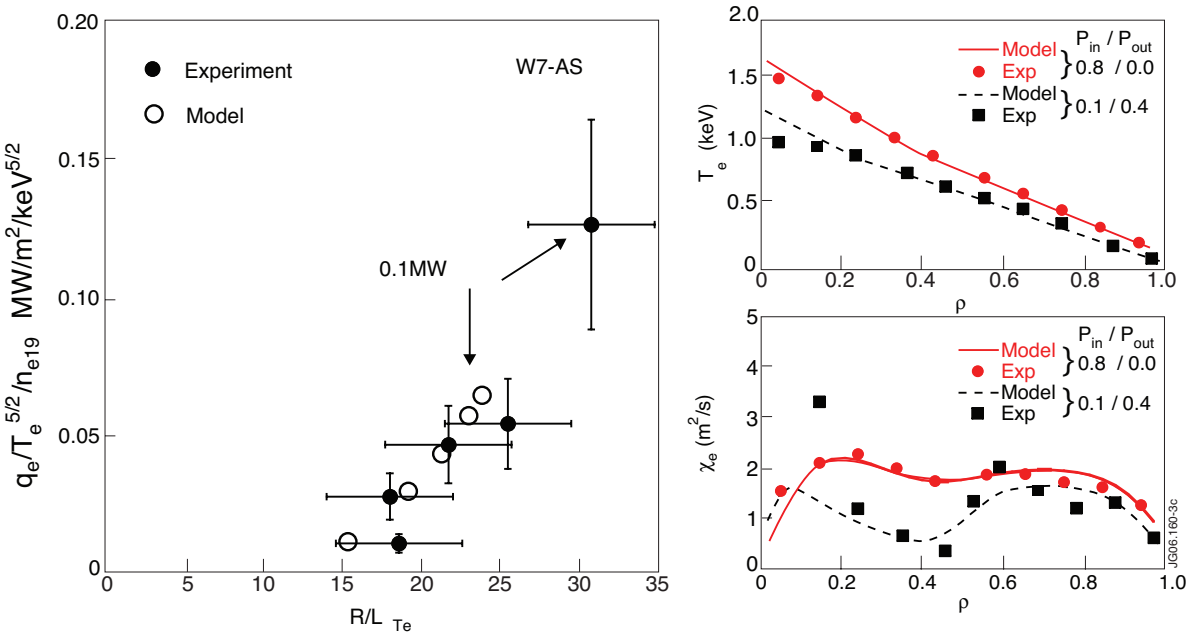

Figure 3: Left plot: electron heat ux versus R/L_{Te}, experimental data and simulations with the empirical mode for W7-AS. Right plot: T_e and χ_e profiles from the simulation and from experiment for 2 cases: 0.8MW on-axis; combination 0.1MW on-axis + 0.4MW off-axis

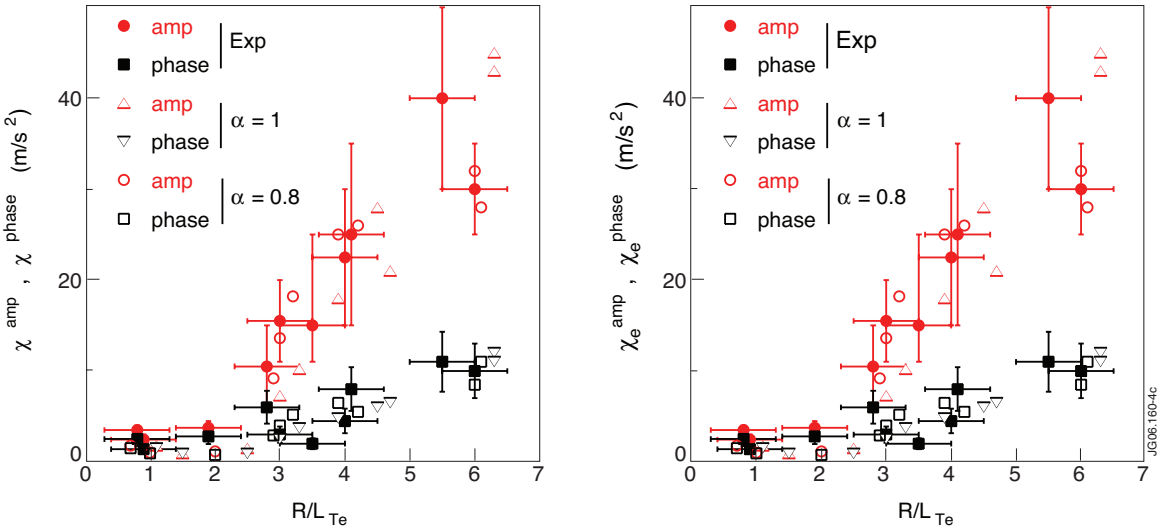

Figure 4: Threshold in ASDEX Upgrade (from [53]).
Left plot: electron heat flux versus R/L_{Te}, experimental data and simulations with the empirical model.The line indicates the growth rate of the TEM at the maximum of $\gamma/k^2_{\perp}$.
Right plot: χ_e^{amp} and χ_e^{phase} versus R/L_{Te}. Experimental data and results from modeling as indicated by the legend.

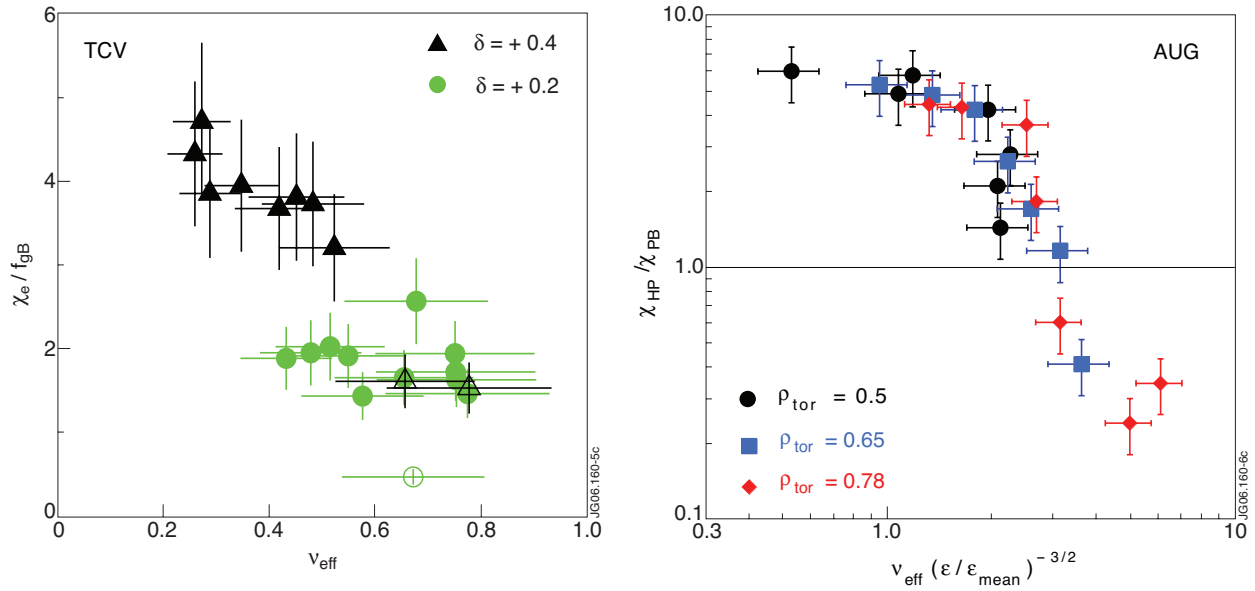

Figure 5: Left plot TCV: Variation of normalised di usivity versus effective collisionality (from [32]). The 3 open symbols indicate ITG dominated discharges. Right plot ASDEX Upgrade: ratio χ_e^{HP} / χ_e^{PB} versus normalised ν_{eff} which shows the strong decrease, interpreted as evidence for a transition from TEM to ITG dominated electron heat transport (from [53]).

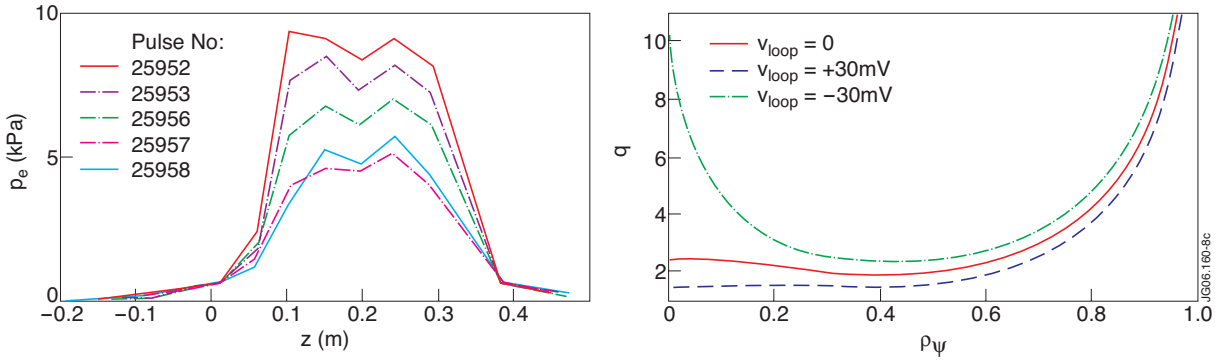

Figure 6: Effect of q profile on eITB in TCV, (after [74]). Left plot: Electron pressure profiles for different shapes of q profiles, three of them being plotted in the right graph.

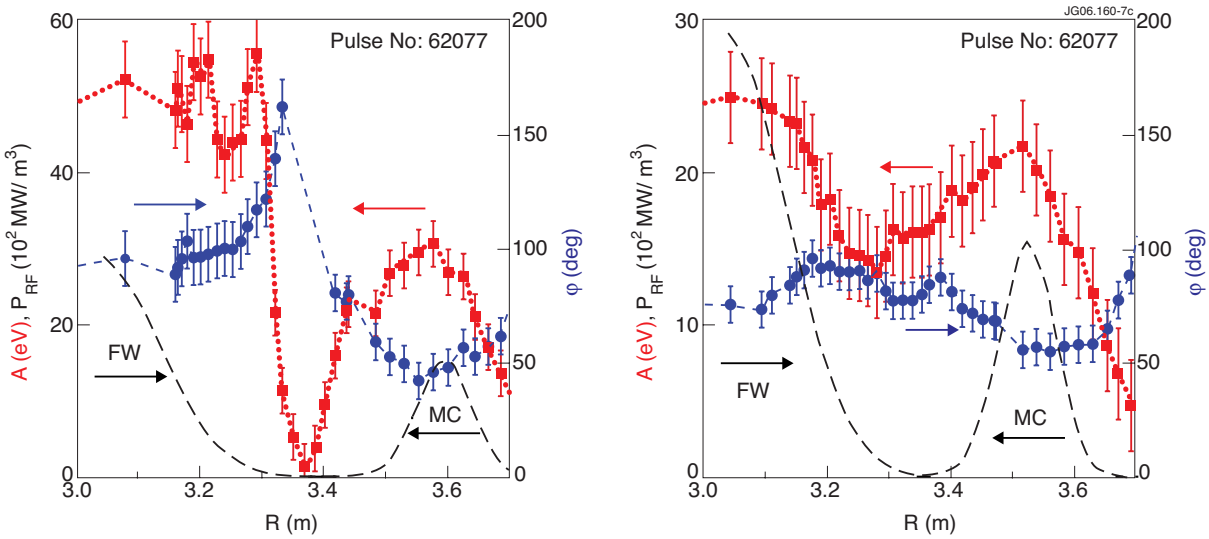

Figure 7: Modulation data with and without ITB in JET, (after [88]).
Left plot: Amplitude (red squares) and phase (blue dots) of the power modulation through an ITB in JET.
Right plot: Same as left plot without ITB.